

A SUPERSONIC, SHOCK FREE NOZZLE, FOR AN EXISTING  
PLASMA GENERATOR AND ITS FACILITIES

by

MERLE KEITH BURKHART

Bachelor of Science

Oklahoma State University

Stillwater, Oklahoma

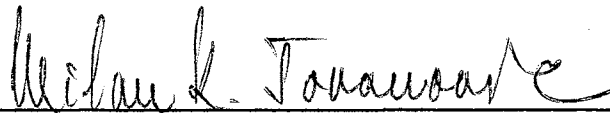
1959

Submitted to the faculty of the Graduate School of  
the Oklahoma State University  
in partial fulfillment of the requirements  
for the degree of  
MASTER OF SCIENCE  
August, 1960

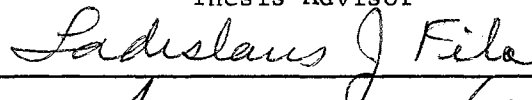
JAN 3 1961

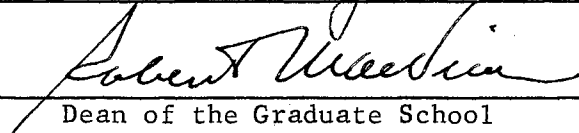
A SUPERSONIC, SHOCK FREE NOZZLE FOR AN EXISTING  
PLASMA GENERATOR AND ITS FACILITIES

Thesis Approved:



Thesis Advisor





Dean of the Graduate School

458057

## PREFACE

Plasma research was introduced at Oklahoma State in 1959. A plasma generator was designed and constructed by Faye C. McQuiston. Until recently the research concerning this generator did not need a nozzle of the type presented in this study. However, due to more extensive research concerning the plasma, it was felt that this nozzle was necessary.

The design of the nozzle in this study is of an experimental nature and will need to be tested under design conditions to determine the practicability of the design.

This study was first begun by considering hydrogen gas to be used to produce the plasma. The hydrogen was to be used regeneratively to regain energy lost by cooling the nozzle walls. Due to fabrication complications encountered in making a high temperature, high pressure nozzle, the study was changed. Argon gas was selected to be used to produce the plasma and the walls were designed to be water cooled.

I wish to express my appreciation for the Honor's Fellowship furnished by the School of Mechanical Engineering which relieved part of the financial burden encountered in this extra year of study.

Recognition also goes to Drs. J. H. Boggs and M. K. Jovanovic for their interest and guidance in this study.

I want to express my sincere appreciation to Professor D. R. Haworth for his helpful assistance concerning this study and its preparation.

The helpful suggestions and assistance of John McCandless and George Cooper of the Mechanical Engineering Laboratory and the work done by the Research Apparatus Development Laboratory were a valuable asset during this study.

Other individuals made helpful suggestions and offered advice worthy of recognition.

I wish to thank my wife, Ramona, for the years of working, waiting, and encouragement which made this goal a reality and for her assistance in preparing this thesis.

## TABLE OF CONTENTS

Chapter	Page
I. INTRODUCTION . . . . .	1
II. THERMODYNAMIC ANALYSIS . . . . .	3
III. MECHANICAL DESIGN. . . . .	7
IV. EXPERIMENTAL OBSERVATIONS AND RESULTS. . . . .	19
V. CONCLUSIONS AND RECOMMENDATIONS. . . . .	30
SELECTED BIBLIOGRAPHY. . . . .	32
APPENDIX	
A. Procedure for Designing a Foelsch Nozzle. . . . .	34
B. Instrument Calibration. . . . .	42

LIST OF TABLES

Table	Page
I. Experimental Data. . . . .	24
II. Properties of Boundary Mach Line for $\gamma = 1.67$ . . .	37

LIST OF PLATES

Plate	Page
I. Nozzle Components . . . . .	11
II. Nozzle Assembly . . . . .	18
III. Test Setup. . . . .	20

## LIST OF FIGURES

Figure	Page
1. Generator Nozzle Plate Details . . . . .	8
2. Expansion Nozzle Details . . . . .	10
3. Mixing Chamber and Nozzle End Plate Details . . . . .	12
4. Cooling Jacket Details . . . . .	14
5. Adaptor Plate Details . . . . .	16
6. Nozzle Assembly . . . . .	17
7. Test Setup . . . . .	21
8. Test Results . . . . .	27
9. Foelsch Nozzle Details . . . . .	36
10. Orifice Calibration Setup . . . . .	43
11. Orifice Calibration Curve . . . . .	45
12. Pressure Gage Calibration Curves . . . . .	46

## CHAPTER I

### INTRODUCTION

Until recent years there has been very little need for the study of materials to withstand extremely high temperatures. With the newly introduced space age, the need arose for a device to produce a continuous flow of high temperature gas for testing purposes.

The plasma generator was developed to produce this high temperature gas flow. In the plasma generator a stream of gas passes through an electric arc and, after expanding in a nozzle, leaves the generator in the form of a jet of high temperature, partially ionized gas called a plasma.

Plasma is the term used to define an electrically neutral mixture of molecules, atoms, ions, and electrons. The combination present depends upon the temperature and the properties of the gas being used. A plasma may be obtained by using any of several types of gases; argon, hydrogen, air, etc.

A method has not yet been developed for measuring, accurately, the temperature of the plasma and, at the present, the temperature can only be estimated very roughly. Extensive studies in this field are being carried on at the present time.

The scope of this thesis involves the design and construction of a convergent-divergent expansion nozzle for plasma research. The



convergent-divergent nozzle is to be used downstream, but not in place, of the existing convergent nozzle in the plasma generator. The purpose of this convergent-divergent nozzle is twofold; to produce a continuous flow of high temperature gas at a high velocity for testing purposes and to aid in the search for a method to measure the temperature in a plasma.

The nozzle was designed for parallel flow at the exit and to produce an exit velocity corresponding to Mach 3.4 using argon gas.

Previous investigation into the subject of high temperature gas flow has not been published extensively. There are, however, a few publications about properties of gases at high temperatures. (1)(2).

An extensive search of the material found no publications concerning the design of supersonic, parallel flow nozzles for extremely high temperatures. The material located pertained mostly to thrust nozzles for rockets and jet aircraft. However, these were not designed to have parallel flow at exit from the nozzles.

Foelsch (3) developed a method of calculation for the contour of a nozzle for parallel flow at exit. A similar method was presented by Beckwith (4). The method by Foelsch has been proven satisfactory for wind tunnel and thrust nozzle design at low temperatures (5).

Much of the information gathered applies to nozzles at the temperatures encountered in a jet engine during chemical combustion (4000°R). Although the argon temperatures would be considerably higher than this (10,000°R), it was decided to use the same basic analysis for the plasma nozzle with slight alterations.

## CHAPTER II

### THERMODYNAMIC ANALYSIS

The investigation was carried out in several steps. First, the flow through a one-dimensional channel was investigated to determine the effect of the Mach number on the area ratio. This investigation of one-dimensional flow, as presented in several texts, e.g., R. C. Binder (6), also involves the relationship of the effect of the Mach number to the temperature, pressure, and density. The effect of heat being transferred from the channel walls was also investigated.

The flow was next considered as isentropic to determine the area ratio, with the properties being assumed constant at the temperature of the gas at inlet to the nozzle. The following properties were determined and tabulated; pressure, Mach number, velocity, temperature, density, area, sonic velocity, and nozzle diameter.

The investigation next assumed isentropic expansions over small increments of the total pressure drop. For each increment, calculations were based on the gas properties for the temperature and pressure at the beginning of the increment. These properties were obtained from reports on the properties of gases at elevated temperatures. (1)(2).

Both hydrogen and argon gas properties were investigated in this manner. The hydrogen properties vary greatly at the temperatures investigated, 5,000° to 10,000° Rankine, while argon properties are nearly constant in this range. This results from the fact that hydrogen gas, being diatomic, will dissociate at these temperatures while argon, a monatomic gas, does not ionize appreciably below 18,000°R.

The effect of the boundary layer was investigated in order to determine its influence on the nozzle area needed for the flow. The assumptions were made that the flow was steady, two-dimensional, and varied according to the equations

$$u/u_s = (y/\delta)^{1/7}$$

and

$$\theta/\theta_s = (y/\delta_t)^{1/7}$$

where

$u$  = velocity at any point for which  $y \leq \delta$ , fps.

$u_s$  = velocity of the free stream, fps.

$y$  = distance measured from the wall, ft.

$\delta$  = boundary layer thickness, ft.

$\delta_t$  = thermal boundary layer thickness, ft.

$\theta$  =  $t - t_w$

$\theta_s$  =  $t_s - t_w$

$t$  = temperature at any distance for which  $y \leq \delta_t$ , °F.

$t_w$  = temperature of the wall, °F.

$t_s$  = temperature of the free stream, °F

The calculations, based upon these assumptions, became very complex. According to A. Melikian (7), concerning his work on a two-dimensional

wind tunnel nozzle, and to information furnished by Dr. Glen Zumwalt of the School of Mechanical Engineering, the boundary layer would be extremely thin in a supersonic nozzle of this type. Because of a very thin boundary layer, the investigation would yield very little useful information. Therefore, further investigation was discontinued.

The effect of the decrease of velocity from the free stream to the wall, and the effect of the temperature drop over this same interval was next considered. The decrease of velocity would tend to increase the area needed to permit the flow of gas that was calculated to be passing through the nozzle. However, since the density of a gas is inversely proportional to the temperature, the decrease in temperature from the free stream to the wall would increase the density and thus allow a greater flow of gas than was calculated by assuming isentropic conditions.

The velocity profile, as well as the temperature profile, were not known in this case. It was assumed that the effect of the increase of density near the wall would offset the decrease in velocity in this same location. The area calculated for isentropic flow was, therefore, used as the area needed for the flow.

The nozzle contour is sometimes calculated by the method of characteristics. This type of design assumes that the properties of the fluid are constant over a finite interval. The assumptions made in the design of a nozzle contour by Foelsch (3) are much less involved than those made in the method of characteristics, and for this reason

the method developed by Foelsch was used to determine the nozzle contour. The equations and method of calculation are shown in Appendix A.

## CHAPTER III

### MECHANICAL DESIGN

The mechanical design of the supersonic nozzle was carried out by using standard engineering practices, materials that were readily obtainable, and with the consideration of fabrication and assembly in mind.

In order to attach the supersonic nozzle to the existing plasma generator designed by Faye C. McQuiston (8) and to attach the generator to the test section, it was necessary to modify the existing generator nozzle plate. The modification included several features:

1. The diameter of the generator nozzle plate was increased from  $6\frac{1}{2}$  inches to 13 inches.
2. For attachment to the test section 6 -  $7/16$ -inch holes were made on a 12-inch diameter.
3. To attach the nozzle assembly to the nozzle plate 6 -  $1/4$ -inch holes on an 8-inch diameter were made.
4. To provide passages for cooling water to the nozzle assembly 8 -  $3/32$ -inch holes on a 4-inch diameter were drilled.

The modified generator nozzle plate is shown in Fig. 1. As in the original design, the modified generator nozzle plate is made of

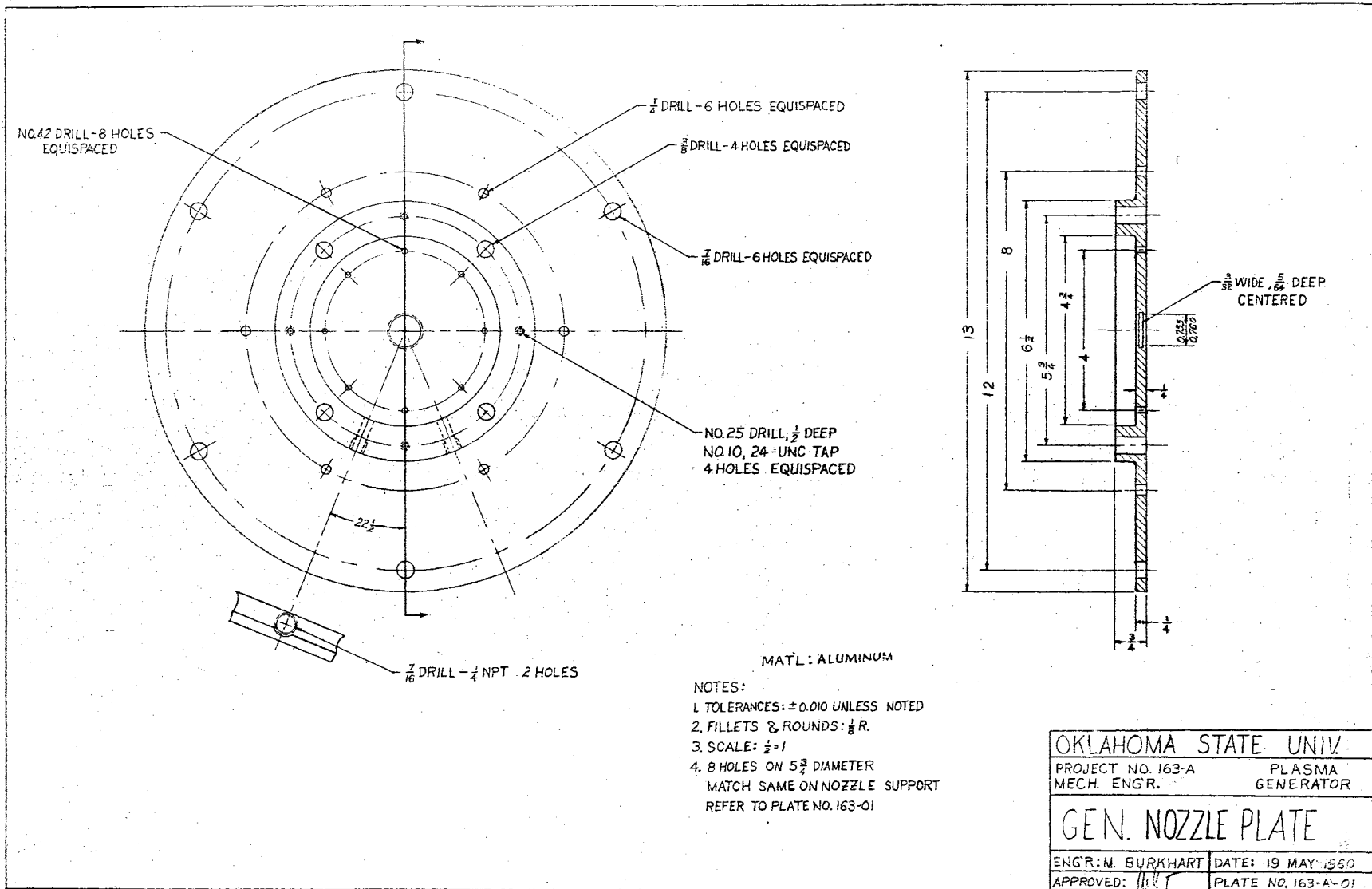


Figure 1. Generator Nozzle Plate Details

32-ST aluminum.

The supersonic nozzle assembly consists of the nozzle, mixing chamber, cooling jacket, nozzle end plate, and the adaptor plate. The individual components are shown in Figs. 2 - 5 and Plate I.

The nozzle is shown in Fig. 2 and was made of copper to facilitate cooling. Copper was chosen because of its high thermal conductivity and because it can be kept from melting by cooling the outer side of the nozzle. The nozzle sides are approximately 1/8-inch thick. The exit end of the nozzle has a groove for an O-ring to seal the water passage around the outside of the nozzle. At the inlet, the nozzle has a double press fit section. This double press fit insures a tight seal between the nozzle and mixing chamber. This seal prevents gas and water leakage.

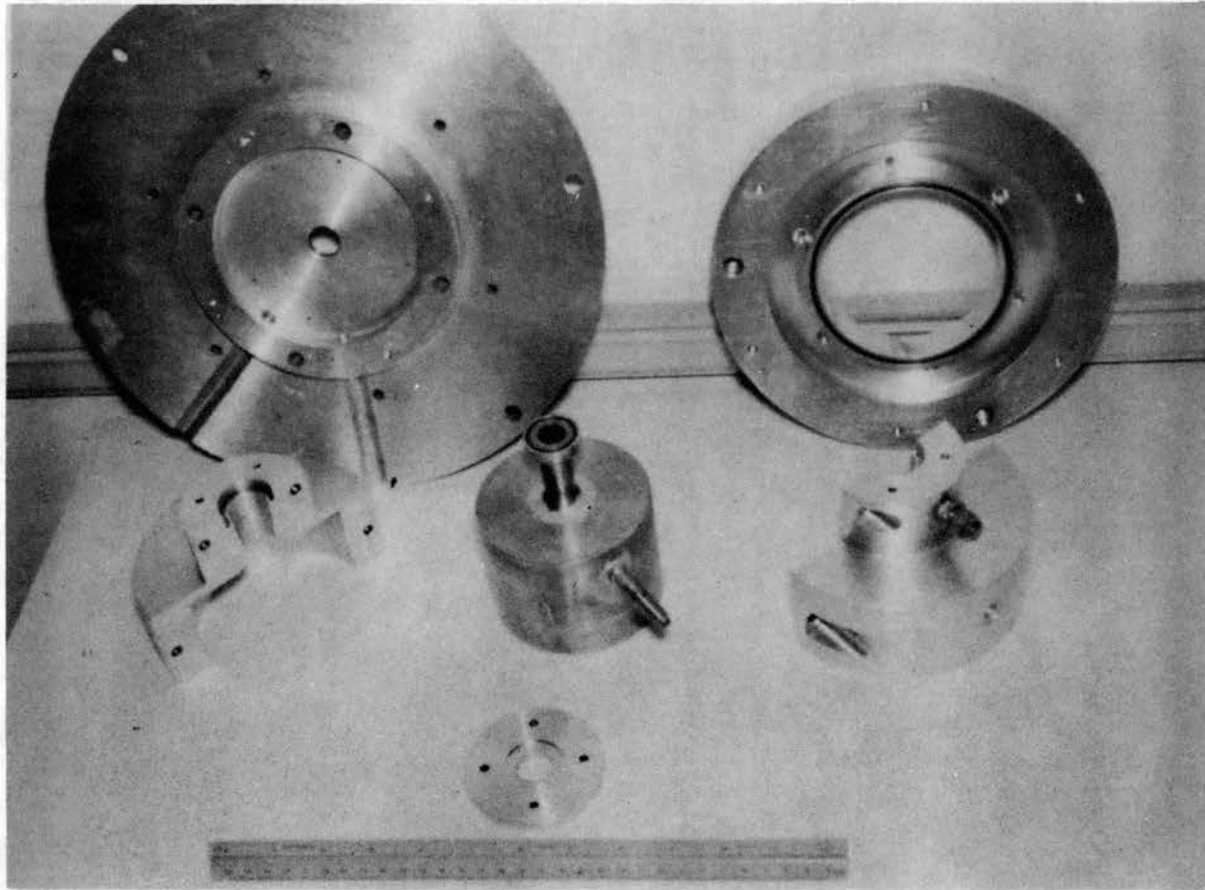
The mixing chamber, Fig. 3, was made of brass and is used to damp the gas swirl as it leaves the convergent nozzle, prior to entry into the supersonic nozzle. The chamber has a groove cut for an O-ring seal against the generator nozzle plate, and also has a double press fit section for the nozzle. A pressure tap located on the top of the mixing chamber will be used for determining the pressure of the gas before entry into the expansion nozzle. The tap is made of brass with an inside diameter of 3/16-inch and outside diameter of 3/8-inch. The tap is threaded on the protruding end to be used for sealing the cooling water passage.

The mixing chamber is held in the center of the cooling jacket passage by three spacers, 120° apart. The spacers are used to insure





PLATE I  
NOZZLE COMPONENTS



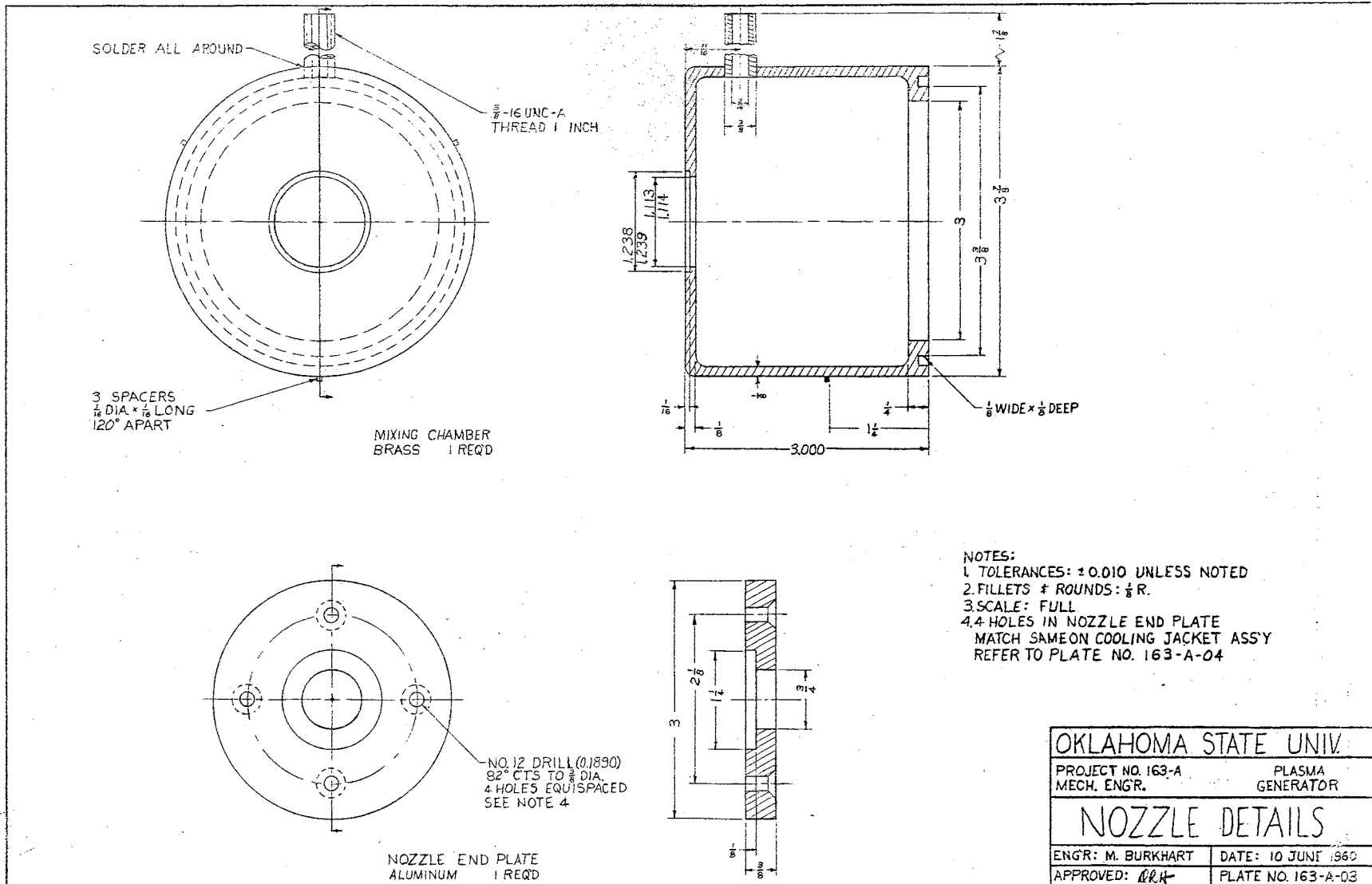


Figure 3. Mixing Chamber and Nozzle End Plate Details

that cooling water will circulate on all sides of the mixing chamber.

The cooling jacket, Fig. 4, was made of 32-ST aluminum. This material was chosen because of its availability and machinability. The cooling jacket is used to provide a water passage approximately 1/16-inch in width outside of the mixing chamber and the nozzle. The jacket had to be made in two parts so that it could be placed around the nozzle and still keep the water passage small.

The two pieces comprising the cooling jacket are held together by 4 screws. A water tap was located in the cooling jacket to allow water to flow through it and then to the drain. The tap is located on top to insure that the passage will be full of water at all times. A 1/8-inch wide and 3/8-inch deep groove was provided at the end of the cooling jacket to allow cooling water to flow freely from all points around the end of the nozzle.

On the front of the cooling jacket, 6 holes on a 5-1/8-inch diameter were tapped for assembly to the adaptor plate. On the other end of the cooling jacket, 4 holes on a 2-1/8-inch diameter were tapped for attachment to the nozzle end plate. A hole, 25/64-inch in diameter, was drilled through the top piece for the pressure tap, and a 3/4-inch spotface was made on the outside to insure a good seal.

The nozzle end plate, Fig. 3, was made of aluminum and is used to locate the nozzle in the center of the cooling jacket passage and for sealing purposes. The plate has 4 holes on a 2-1/8-inch diameter to match those in the cooling jacket, and seats against a neoprene O-ring in the end of the nozzle.

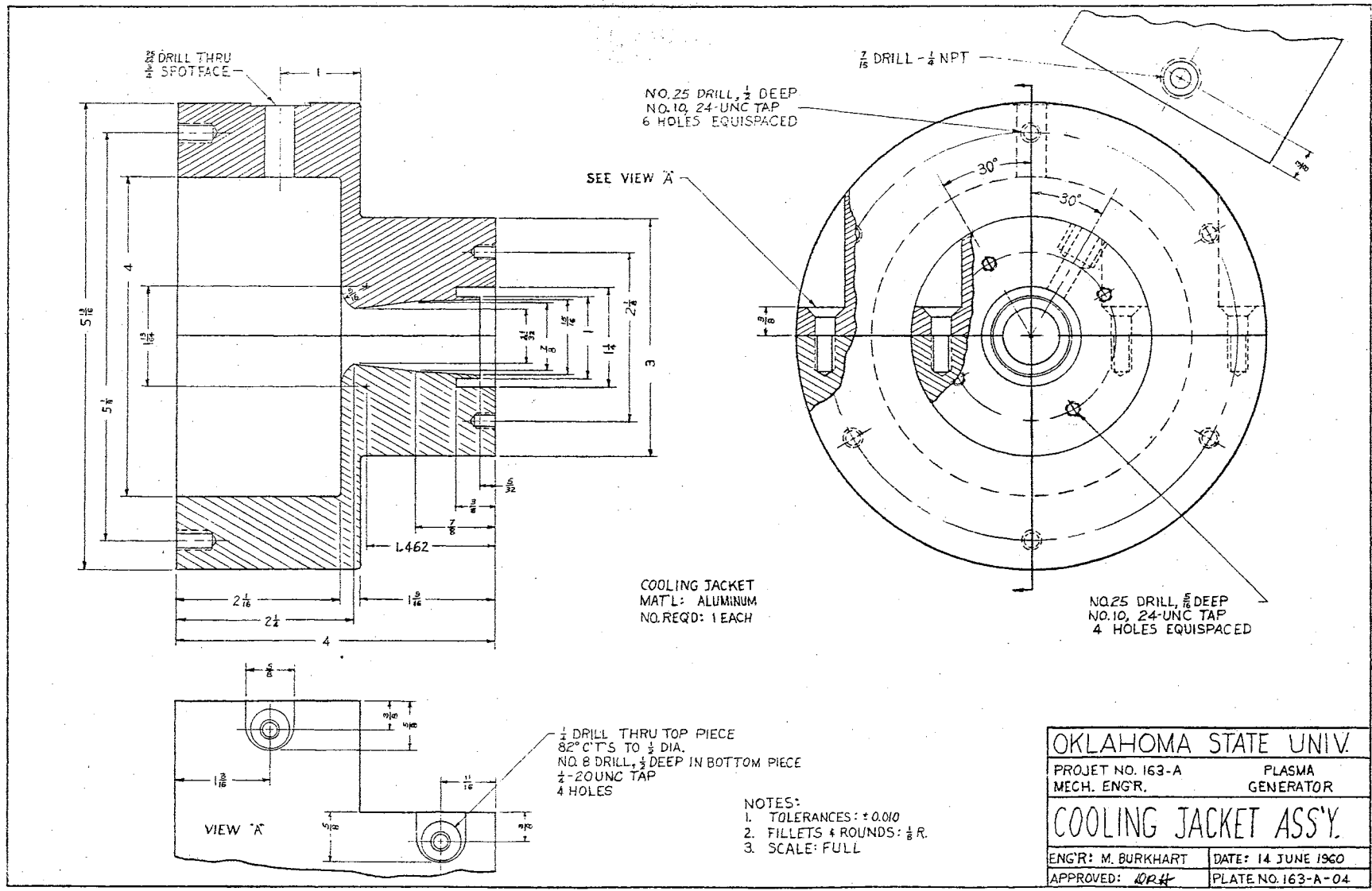


Figure 4. Cooling Jacket Details

The adaptor plate, Fig. 5, is used to connect the cooling jacket to the generator nozzle plate. The adaptor plate is used also as part of the water passage at the beginning of the mixing chamber. It has 6 tapped holes on an 8-inch diameter to allow attachment to the generator nozzle plate and 6 holes on a 5-1/8-inch diameter to match those on the cooling jacket. A circular groove 7/8-inch wide and 1/2-inch deep was made to allow clearance for the existing bolts on the plasma generator. A groove was made for an O-ring seal between the adaptor plate and the generator nozzle plate.

The supersonic nozzle assembly and the modified generator nozzle plate are shown assembled in Fig. 6 and Plate II. By pressing the nozzle into the allotted place in the mixing chamber, attaching the end plate and adaptor plate to the cooling jacket, and placing these around the nozzle and mixing chamber, the water passages were kept open but the O-rings were not yet pressed to insure good seals. The supersonic nozzle assembly was then attached to the generator nozzle plate. By tightening the screws holding the adaptor plate to the generator nozzle plate, the neoprene O-ring seals were pressed against mating parts to effect the seal.

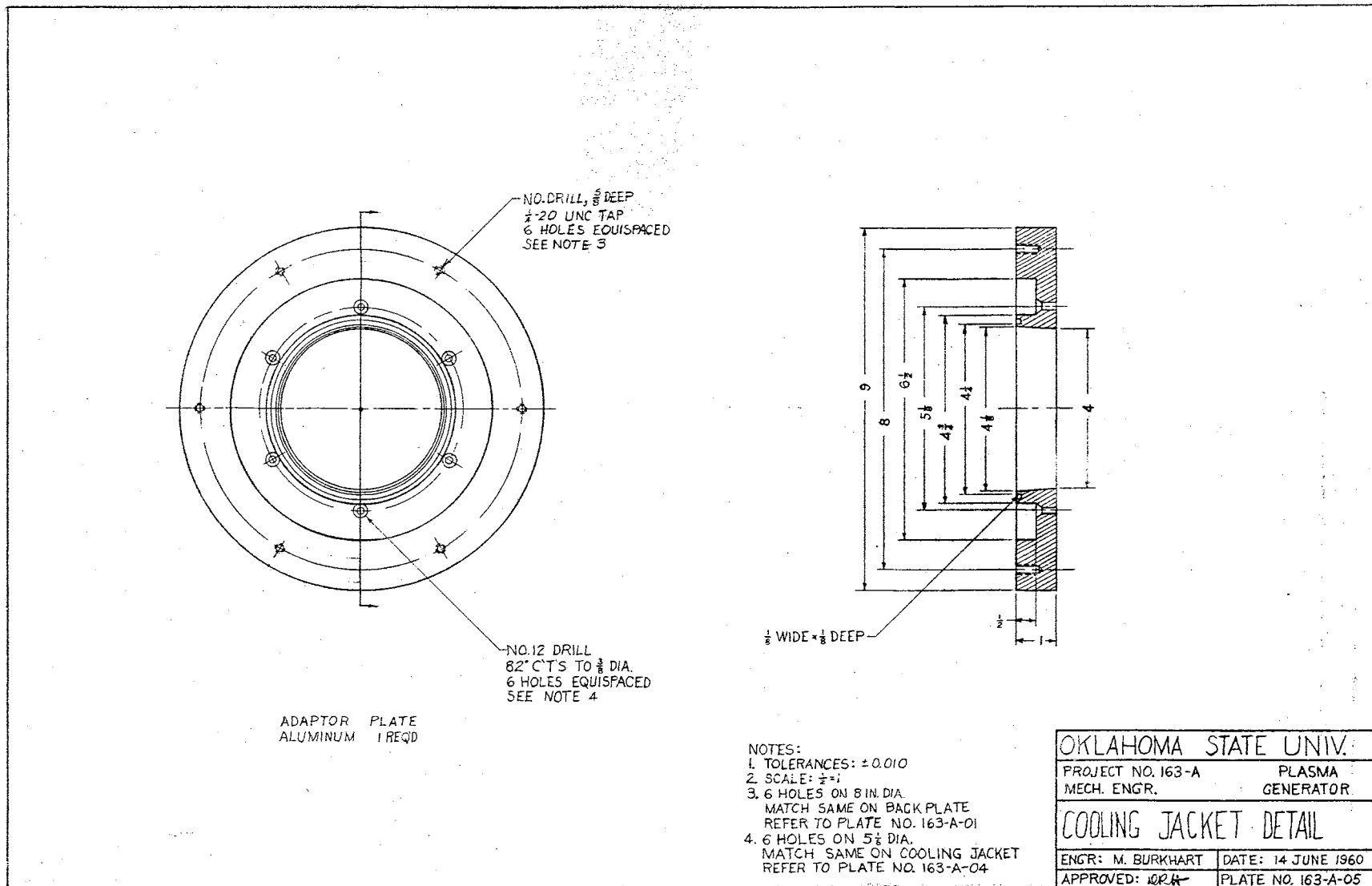


Figure 5. Adaptor Plate Details

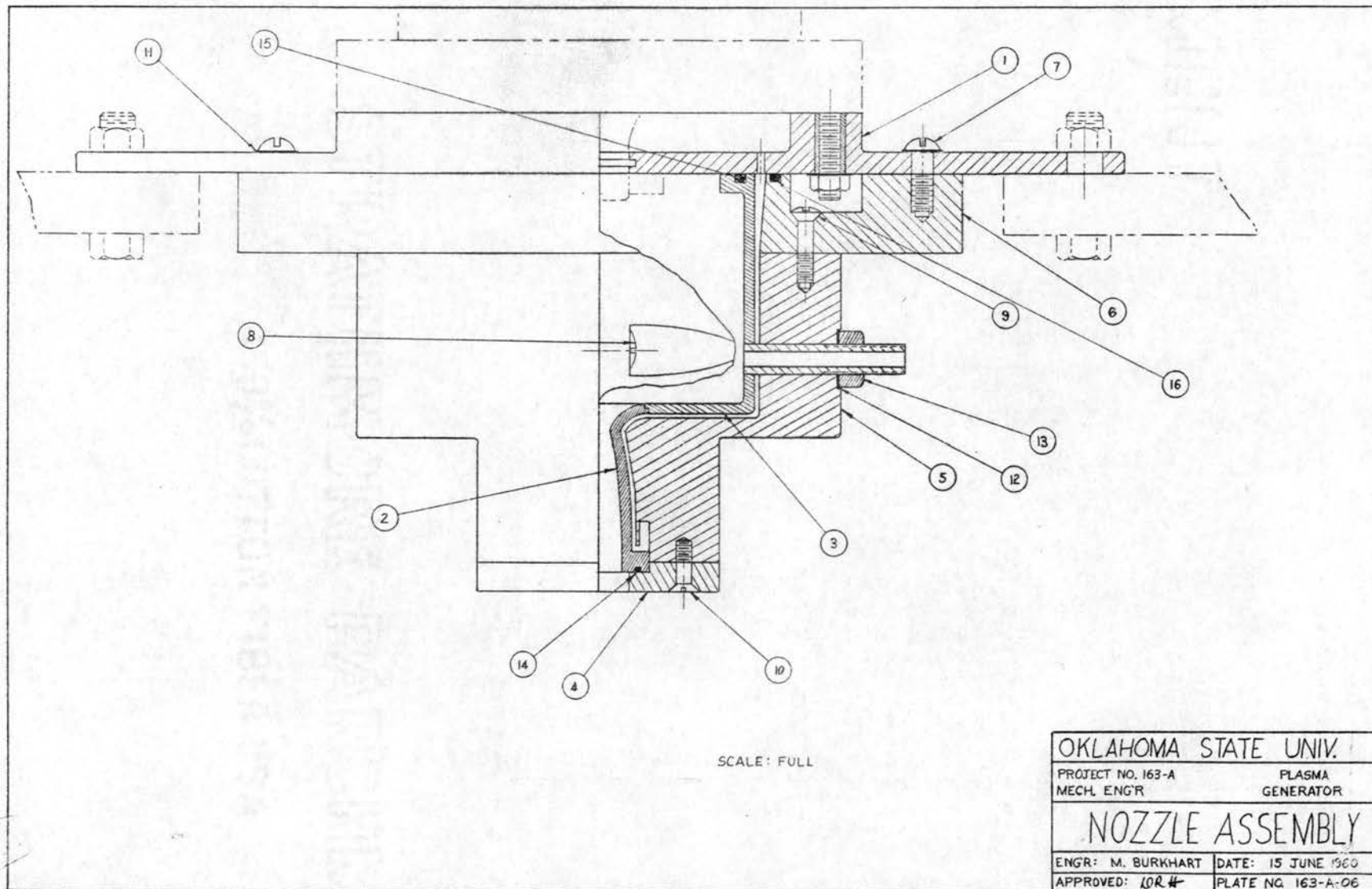
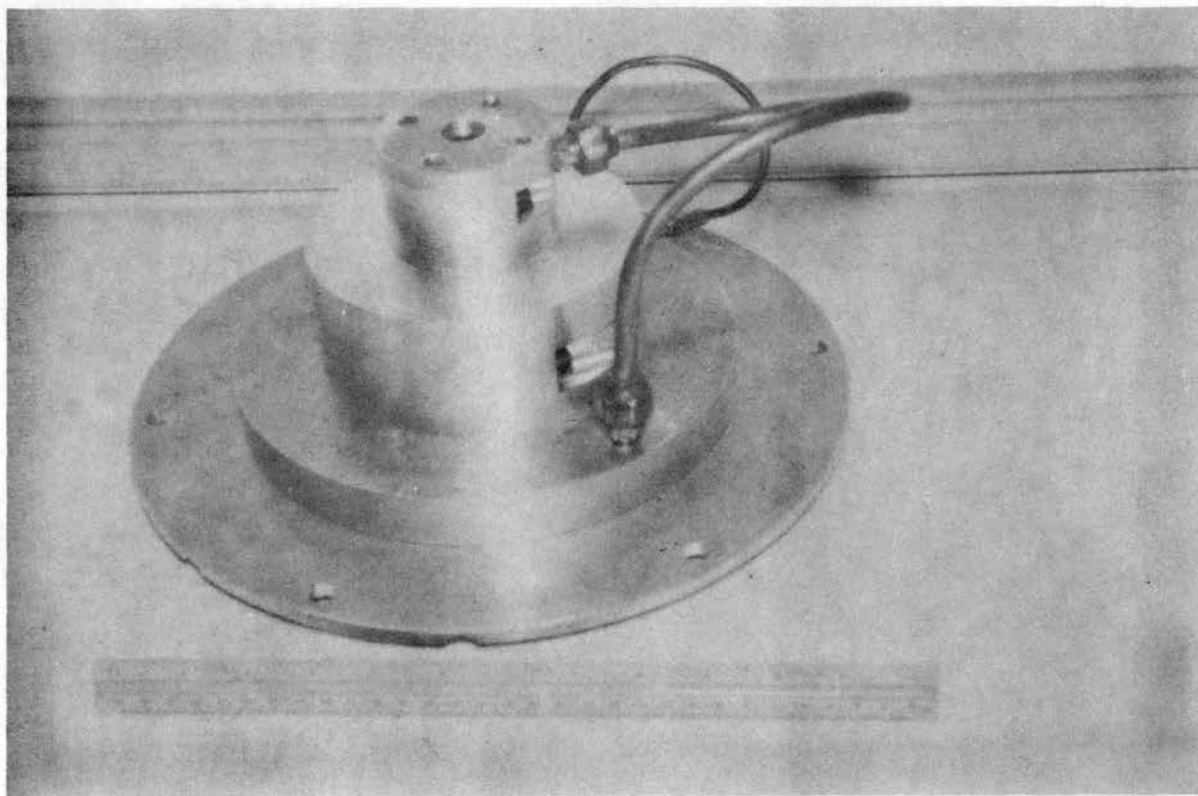


Figure 6. Nozzle Assembly



PLATE II  
NOZZLE ASSEMBLY



## CHAPTER IV

### EXPERIMENTAL OBSERVATIONS AND RESULTS

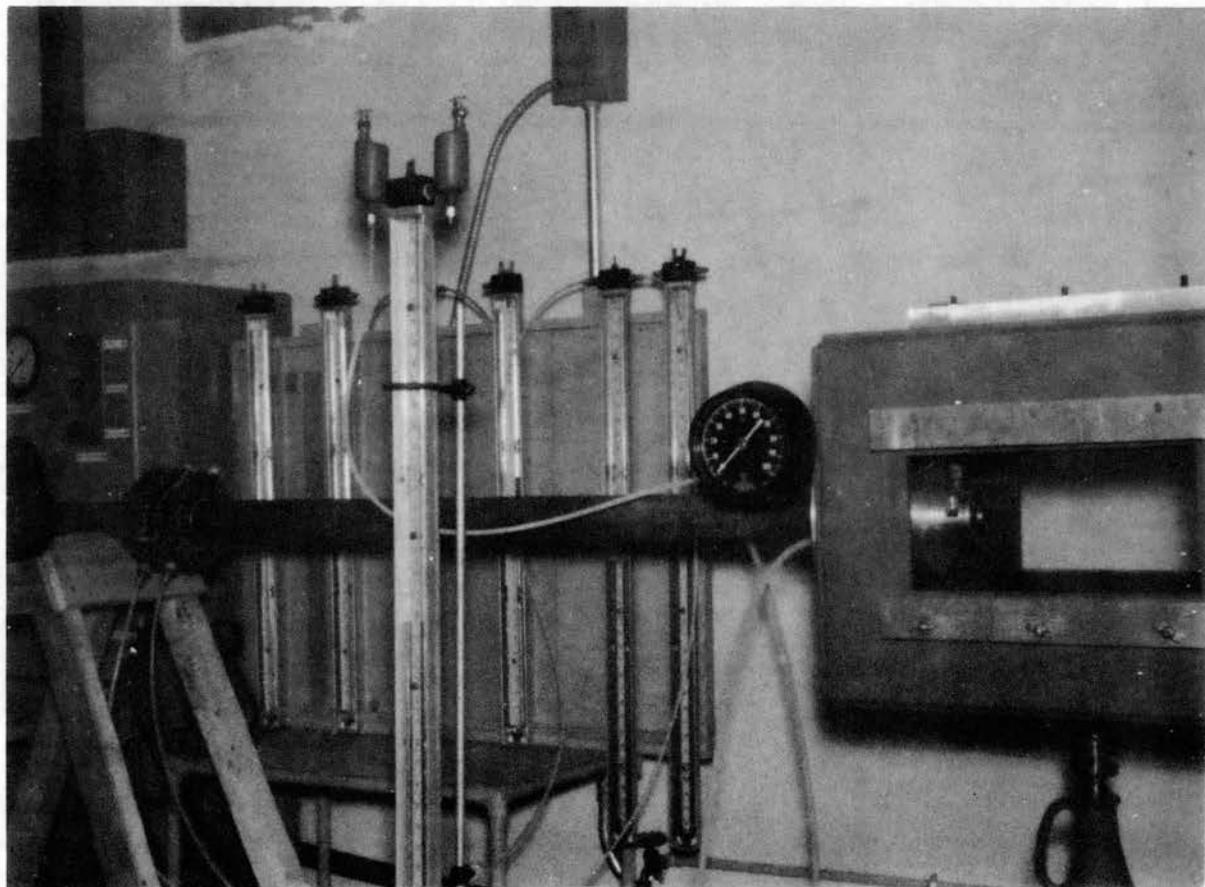
The supersonic nozzle components were assembled using 3M weatherstripping compound for sealing the two halves of the cooling jacket and for a seal between the nozzle end plate and the cooling jacket.

The facilities to test the supersonic nozzle using argon gas and discharging into a vacuum system were not available at the time that the nozzle was completed. As an alternative, the nozzle assembly was tested using air and discharging to the atmosphere. The mass flow rate of air through the nozzle was experimentally determined for mixing chamber pressures from 15.56 to 40.52 psia. The measured flow rates were compared to the calculated flow rates based on the mixing chamber and nozzle exit pressures and the geometry of the nozzle.

The test setup is shown schematically in Fig. 7 and a photograph of the setup is shown in Plate III. A regulator was used to stabilize the flow into the mixing chamber since the compressed air supply pressure varied as much as 15 psi.

The mass flow rate entering the nozzle was measured by means of a calibrated orifice installed in the air line upstream of the nozzle. The pressure taps in the flanges of the orifice were connected to a manometer to measure the differential pressure across the orifice. A

PLATE III  
TEST SETUP



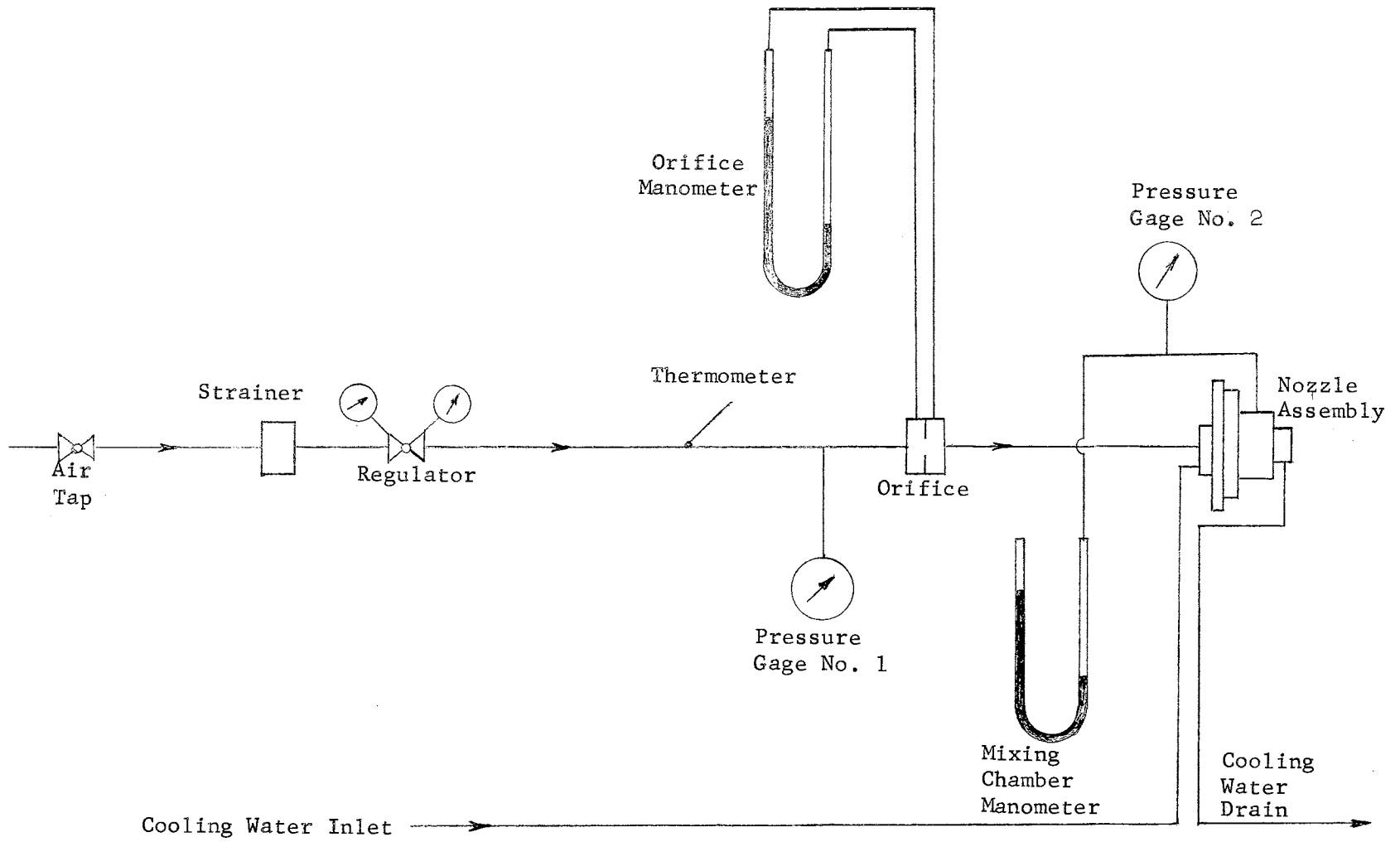


Figure 7. Test Setup

gage was installed immediately upstream of the orifice to determine the pressure of the air at the orifice. The slight variation of the pressure between this location and the orifice plate was assumed negligible. A pressure gage was also located on the pressure tap in the mixing chamber. At low pressures, this gage was exchanged for a mercury manometer to increase the accuracy of the readings. The calibration data for the orifice meter and the pressure gages are contained in Appendix B.

A solid aluminum plate with holes drilled to allow water flow into the nozzle passages and with a connection for the air line was used in place of the generator nozzle plate of the plasma generator.

The temperature of the air in the piping was measured with a thermometer inserted in the flow immediately upstream of the orifice pressure gage.

An audible instability in the flow coming from the nozzle was noticed at chamber pressures above 25 psia. This instability was attributed to the existence of a shock wave in the divergent portion of the nozzle. Analysis showed that a shock wave will exist when the pressure ratio across the nozzle is such that the flow is not completely expanded and when the nozzle does not act as a venturi with isentropic expansion and compression taking place.

During the test, runs at 11 different flow rates were made. During each run the pressure of the air at the orifice, the differential pressure across the orifice, and the chamber pressure were recorded.

The values of the differential pressure across the orifice,

orifice pressure, and line temperature were used to calculate the mass flow rate of air through the orifice. The orifice calibration curve (Fig. 11 in Appendix B) gives the flow coefficient at different Reynolds numbers. The corrected readings and the calculated results are shown in Table I.

The mass flow rate of air through the nozzle was calculated using the following relation (9):

$$\rho_a \bar{v}_a = \sqrt{\frac{2\gamma g_c}{\gamma-1} P_o \rho_o \left[ \left(\frac{P_a}{P_o}\right)^{2/\gamma} - \left(\frac{P_a}{P_o}\right)^{(\gamma+1)/\gamma} \right]} \quad (1)$$

where  $\rho_a$  = Density at point a, lb<sub>m</sub>/ft<sup>3</sup>  
 $\bar{v}_a$  = Velocity at point a, fps.  
 $P_o$  = Stagnation pressure, psfa  
 $\rho_o$  = Stagnation density, lb<sub>m</sub>/ft<sup>3</sup>  
 $P_a$  = Pressure at point a, psfa  
 $\gamma$  = Ratio of specific heats, 1.4 for air.

Equation (1) is the mass flow rate per unit area assuming isentropic flow and a negligible elevation change.

To determine the mass flow rate at point a, equation (1) was multiplied by  $A_a$  to yield

$$\dot{m} = \rho_a \bar{v}_a A_a = A_a \sqrt{\frac{2\gamma g_c}{\gamma-1} P_o \rho_o \left[ \left(\frac{P_a}{P_o}\right)^{2/\gamma} - \left(\frac{P_a}{P_o}\right)^{(\gamma+1)/\gamma} \right]} \quad (2)$$

where  $\dot{m}$  = Mass flow rate, lb<sub>m</sub>/sec  
 $A_a$  = Area of nozzle at point a, ft<sup>2</sup>.

TABLE I  
EXPERIMENTAL DATA

Run No.	Orifice Manometer (in. H <sub>2</sub> O)	Orifice Pressure (psia)	Chamber Pressure (psia)	Mass Flow Rate (lb <sub>m</sub> /sec)
1	33.3	41.52	40.52	0.0620
2	32.1	39.52	38.52	0.0595
3	28.5	35.52	34.52	0.0532
4	27.5	34.52	33.02	0.0516
5	23.0	28.52	27.52	0.0430
6	20.6	25.52	25.60	0.0386
7	18.5	23.52	22.90	0.0352
8	14.3	19.02	18.42	0.0279
9	10.0	16.52	16.63	0.0219
10	5.9	15.52	15.56	0.0153

Barometric pressure: 29.54 in. Hg.

Temperature of air stream: 82°F

For flow at the nozzle throat the formula becomes

$$\dot{m} = A_t \sqrt{\frac{2\gamma g_c}{\gamma-1}} P_o \rho_o \left[ \left(\frac{P_t}{P_o}\right)^{2/\gamma} - \left(\frac{P_t}{P_o}\right)^{(\gamma+1)/\gamma} \right] \quad (3)$$

where  $A_t$  = Area of the throat.

For choked flow at the throat the value of  $P_t/P_o$  is 0.5283.

Substituting this value of  $P_t/P_o$ ,  $\gamma = 1.4$ , and  $g_c = 32.174 \text{ lb}_m\text{-ft}/\text{lb}_f\text{-sec}^2$  into equation (3) for the flow rate at the throat yields

$$\dot{m} = 3.87 A_t \sqrt{P_o \rho_o} \quad (4)$$

By using the perfect gas relation  $\rho = P/RT$  equation (4) becomes

$$\dot{m} = (3.87 A_t / \sqrt{RT_o}) P_o \quad (5)$$

which shows that, for a constant stagnation temperature, the mass flow rate varies linearly with the stagnation pressure if the nozzle is choked.

Since the cross sectional area of the 2-inch air line used was large, the velocity of the air stream was small. The velocity of the flow was calculated by

$$\bar{V} = \frac{\dot{m}}{\rho A} = \frac{4\dot{m}RT}{\pi D^2 P} \quad (6)$$

At the highest flow rate used in the test the velocity was 137 feet per second. At this velocity the variation between static and stagnation pressure would be small; therefore, the chamber pressure was considered to be the stagnation pressure.

For a nozzle exit pressure of 29.54 inches of mercury, 14.52 psia,



the flow becomes choked with a stagnation pressure of 14.77 psia. As the stagnation pressure rises above 14.77 psia the flow is choked and the mass rate is a linear function of the stagnation pressure. As the pressure decreases from 14.77 psia to 14.52 psia the flow rate decreases to zero.

The stagnation pressure of 14.77 psia at which the flow becomes choked was determined by analyzing isentropic, one-dimensional flow through the nozzle.

At choked conditions the flow will reach sonic velocity at the throat. The throat to entrance conditions and also the throat to exit conditions were used to determine the relationship of the entrance to exit conditions.  $A^*$  is defined as the area at which sonic velocity is obtained. When choking occurs,  $A^*$  will be equal to  $A_t$ . The ratio of the exit to throat area ( $A_E/A_t$ ) was known to be 3.908. Therefore

$$A_E/A^* = A_E/A_t = 3.908 .$$

Corresponding to this area ratio in the air tables (10), the ratio of the stagnation to exit pressure was found to be 0.9845. The stagnation pressure for an exit pressure of 14.52 psia was calculated to be 14.77 psia.

The measured and calculated mass flow rates versus stagnation pressure in the mixing chamber are plotted in Fig. 8. The close agreement of the experimental data to the calculated values in the upper region shows that the flow followed the anticipated trend.

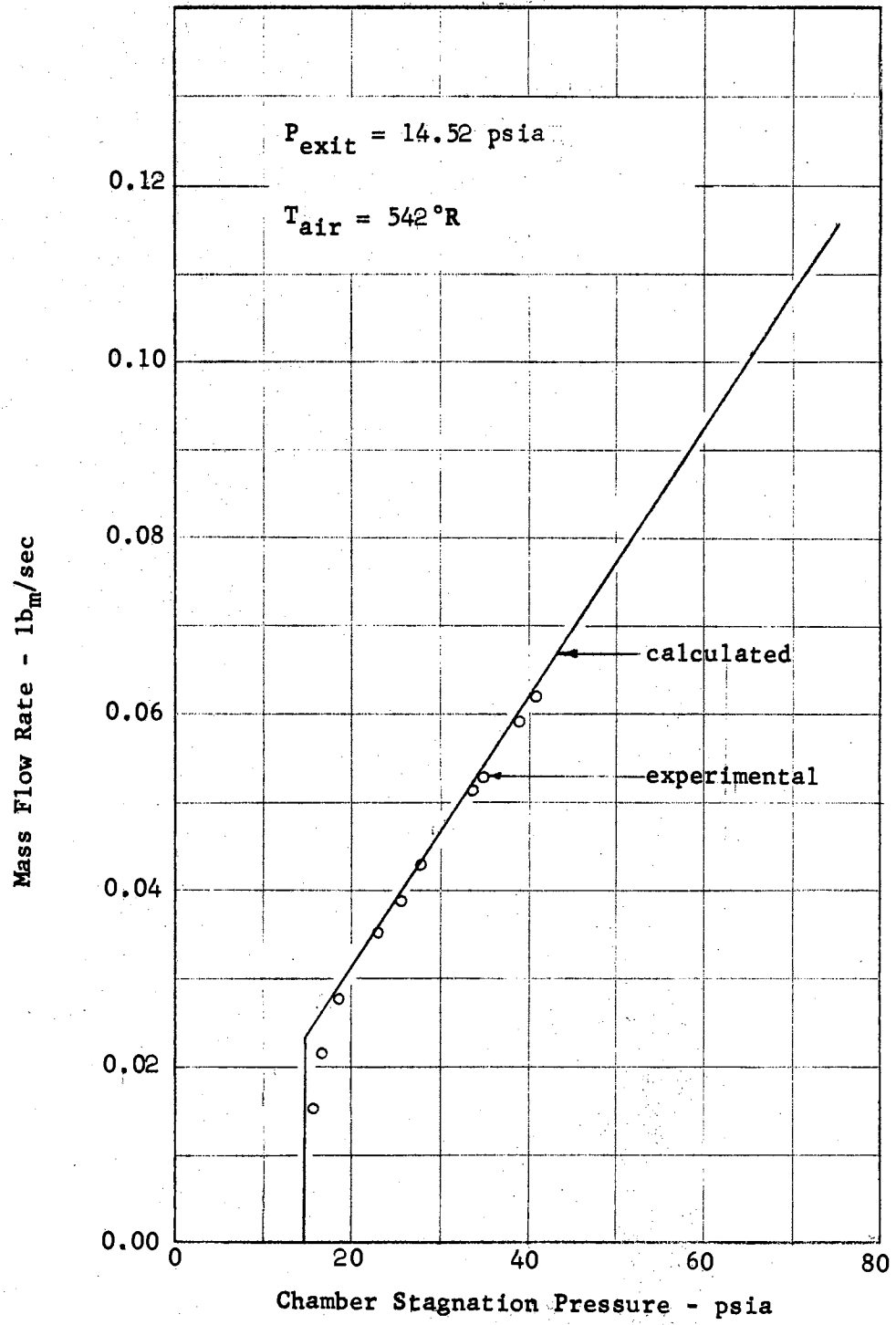


Figure 8. Test Results

The small deviations of the points above 18 psia were probably due to experimental error and to the presence of a boundary layer in the nozzle which was not considered in the calculations. The deviations of the experimental values became pronounced below 18 psia stagnation pressure. The experimental data indicated that choking did not occur at 14.77 psia, but that the choking effect was delayed until a higher stagnation pressure was reached.

The deviations in the lower range may have been the result of the boundary layer effect. At the lower flow rates and pressures, the boundary layer is thicker than at higher flow rates and pressures. It is possible that the boundary layer at the throat did not vary appreciably throughout the test and remained relatively thin while the boundary layer in the diverging section became thicker at lower flow rates. The growth of the boundary layer in the divergent portion would effectively decrease the exit area of the nozzle. Before choking occurs, the nozzle acts as a venturi. The previously mentioned delayed choking effect can be visualized by considering the effect of the exit to throat area relation of a venturi meter. As the area ratio is decreased, the pressure ratio must be increased to induce choking of the venturi. The above described phenomena could account for the deviations of the measured flow rates from the calculated values.

The presence of water vapor in the air flow may have contributed to the deviations of the experimental results. There was no allowance made in the calculations for the presence of water vapor in the

air although a strainer was used immediately upstream of the regulator to eliminate water droplets present in the air stream.

## CHAPTER V

### CONCLUSIONS AND RECOMMENDATIONS

The supersonic nozzle assembly worked satisfactorily as shown by the close agreement between the two curves of Fig. 8. This result shows also that the boundary layer has a slight influence at the higher pressures.

The supersonic nozzle assembly will have to be tested under the conditions for which it was designed, in order to determine the accuracy of the design of the nozzle contour.

The following are some of the conclusions drawn from the design and test of this convergent-divergent nozzle.

1. The design proved satisfactory using air as the gas instead of argon.
2. The water passages were open to the flow of cooling water through the jacket.
3. The boundary layer had some influence under the conditions of this test.

The following are recommendations for further testing the nozzle before its use in experiments:

1. Test the nozzle assembly under actual design conditions to determine the pressure drop through the nozzle for shock free flow at supersonic velocities.

2. If possible, determine the shape of the flow at the nozzle exit to check if it is parallel under design conditions.

3. Check the cooling ability of the nozzle assembly under design conditions and determine the influence of different cooling water flow rates.

Tests other than these can be made on this convergent-divergent nozzle. However, the ones recommended above are felt to be the most important since these should be known to check the validity of this design.

The nozzle may need to be modified for later experiments in which it will be used, but the present design is thought to be satisfactory for its use in determining a method of measuring the temperatures in the plasma jet and for testing purposes.

#### SELECTED BIBLIOGRAPHY

1. Ducati, A. C. and Cann, G. L. "Propulsive Properties of High Intensity Plasma Jets." Giannini Research Laboratory Technical Report No. 9, AFOSR (ARDC) Project No. 37507, February 21, 1958.
2. Gross, R. A. and Eisen, C. L. "Some Properties of a Hydrogen Plasma." AFOSR Technical Note 59-388, Contract No. AF 49(638)-15, ASTIA AD 216770, June, 1959.
3. Foelsch, Kuno. "The Analytic Design of an Axially Symmetric Laval Nozzle for a Parallel and Uniform Jet." Journal of the Aeronautical Sciences, Vol. 16, No. 3, 1949, pp. 161-166, 188.
4. Beckwith, Ivan E. and Moore, John A. "An Accurate and Rapid Method for the Design of Supersonic Nozzles." NACA Technical Note 3322, Langley Aeronautical Laboratory, Langley Field, Virginia.
5. Landsbaum, Ellis M. "Contour Nozzles." American Rocket Society Journal, Vol. 30, No. 3, March, 1960, pp. 244-250.
6. Binder, R. C., Ph. D. Advanced Fluid Dynamics and Fluid Machinery. New York: Prentice-Hall, Inc., 1951, pp. 67-73, 77-87.
7. Melikian, A. "Design of a Supersonic Wind Tunnel for Mach Numbers 2.0 to 3.5 With Variable Second Throat." M. S. Thesis, Oklahoma State University, May, 1960.
8. McQuiston, Faye C. "Design and Operation of a Plasma Generator Using Argon as the Stabilizing Gas." M. S. Thesis, Oklahoma State University, August, 1959.
9. Lee, John F. and Sears, Francis W. Thermodynamics. Readings, Massachusetts: Addison-Wesley Publishing Company, Inc., July, 1956, p. 244.
10. Keenan, Joseph H. and Kaye, Joseph. Gas Tables. New York: John Wiley and Sons, Inc., September, 1950, p. 139.

11. Jovanovic, Milan K. "Plasma Research." Progress Report for Oklahoma State University from February 1, 1959 to June 15, 1959, Institutional Project No. 163.
12. Liepmann, H. W. and Roshko, A. Elements of Gasdynamics. Galcit Aeronautical Series. New York: John Wiley and Sons, Inc., March, 1958, pp. 124-130, 292-295, 301-304.
13. Saunders, O. A. and Calder, P. H. "Heat Transfer in a Nozzle at Supersonic Speeds." Engineering, August 29, 1952.
14. Shapiro, Ascher H. The Dynamics and Thermodynamics of Compressible Flow, Vol. I, New York: The Ronald Press Co., 1954, pp. 1-18, 41-43, 265-278, 507-508, 695.
15. Simmons, Frederick S. "Analytic Determination of the Discharge Coefficient of Flow Nozzles." NACA Technical Note No. 3447.



## APPENDIX A

### PROCEDURE FOR DESIGNING A FOELSCH NOZZLE

The supersonic nozzle was designed according to a method set up by Kuno Foelsch (3).

The following equations were used to calculate some of the properties needed for calculation of the nozzle contour:

$$\tau_p^2 = \frac{1}{M_p^2} \left[ \frac{2}{\gamma-1} + \frac{\gamma-1}{\gamma+1} M_p^2 \right] (\gamma+1) \sqrt{2(\gamma-1)}$$

$$\psi_p = \frac{1}{2} \left[ \sqrt{\frac{\gamma+1}{\gamma-1}} \tan^{-1} \sqrt{\frac{\gamma-1}{\gamma+1}} (M_p^2 - 1) - \tan^{-1} \sqrt{M_p^2 - 1} \right]$$

where  $\tau_p$  = Ratio of the diameter  $D_p$ , at any point "p" between points "a" and "e", to the throat diameter  $D_{th}$ .

$\psi_p$  = Expansion angle at any point downstream of the throat ( $\frac{1}{2}$  of the Prandtl-Meyer function). (12).

$\gamma$  = Ratio of specific heats.

$M_p$  = Mach number at any point downstream of the throat.

The design of the contour was carried out in a few steps using Table II on page 37. The steps for the calculation are as follows:

1. Select the desired Mach number at the exit ( $M_e$ ).
2. Determine the diameter of the throat and exit by one-dimensional isentropic functions.
3. Find the following:

a)  $\sqrt{M_e^2 - 1}$

- b)  $\psi_e$  (from Table II)
- c)  $\tau_e$  (from Table II)
- d)  $\omega = \frac{1}{2}\psi_e = \psi_a = \theta_a$
- e)  $\sqrt{M_a^2 - 1}$  (from Table II, using  $\psi_a$ )
- f)  $\tau_a$  (from Table II, using  $\psi_a$ )

4. Solve for  $X_0$ :

$$X_0 = \frac{D_e}{2\tau_e} \left[ \cot \omega - \frac{\tau_a \cos \omega/2 - 1}{2 \cos \omega/2 (\sin \omega/2 + \cos \omega/2)} \right]$$

where  $D_e = \text{exit diameter} = 2 y_e$ .

5. Solve for the coordinates of points from a to e, using the following procedure.

- a) Choose a value of  $\sqrt{M_p^2 - 1}$  between the values obtained from a and e.
- b) Read values of  $\psi_p$  and  $\tau_p$  from Table II.
- c) Find value of  $\theta_p = \psi_e - \psi_p$
- d) Solve for  $F(\theta_p)$ :

$$F(\theta_p) = \left[ \sin^2 \theta_p + 2(\cos \theta_p - \cos \omega)(\sin \theta_p \sqrt{M_p^2 - 1} + \cos \theta_p) \right]^{1/2}$$

e) Solve for  $y_p$ :

$$y_p = \frac{D_e}{4 \sin \omega/2} (\tau_p / \tau_e) [F(\theta_p)]$$

f) Solve for  $\bar{x}_p$ :

$$\bar{x}_p = \left[ \frac{D_e}{4 \sin \omega/2} (\tau_p / \tau_e) \right] \left[ \frac{1 + (\cos \theta_p \sqrt{M_p^2 - 1} - \sin \theta_p) F(\theta_p)}{\sin \theta_p \sqrt{M_p^2 - 1} + \cos \theta_p} \right]$$

g) Determine  $x_p$ :

$$x_p = \bar{x}_p - x_0$$

6. After determining coordinates of an adequate number of points between, and including, points a and e, find the length of the straight section ( $\lambda$ ), and radius (R) of arc section of nozzle:

$$\lambda = R = \frac{D_e (\tau_a \cos \omega/2 - 1)}{4 \tau_e \sin \omega/2 (\cos \omega/2 + \sin \omega/2)}$$

7. Solve for coordinates of point d:

$$x_d = R \sin \omega$$

$$y_d = y_{th} + R (1 - \cos \omega), \text{ where } y_{th} = \text{throat radius} = \frac{D_e}{2 \tau_e}$$

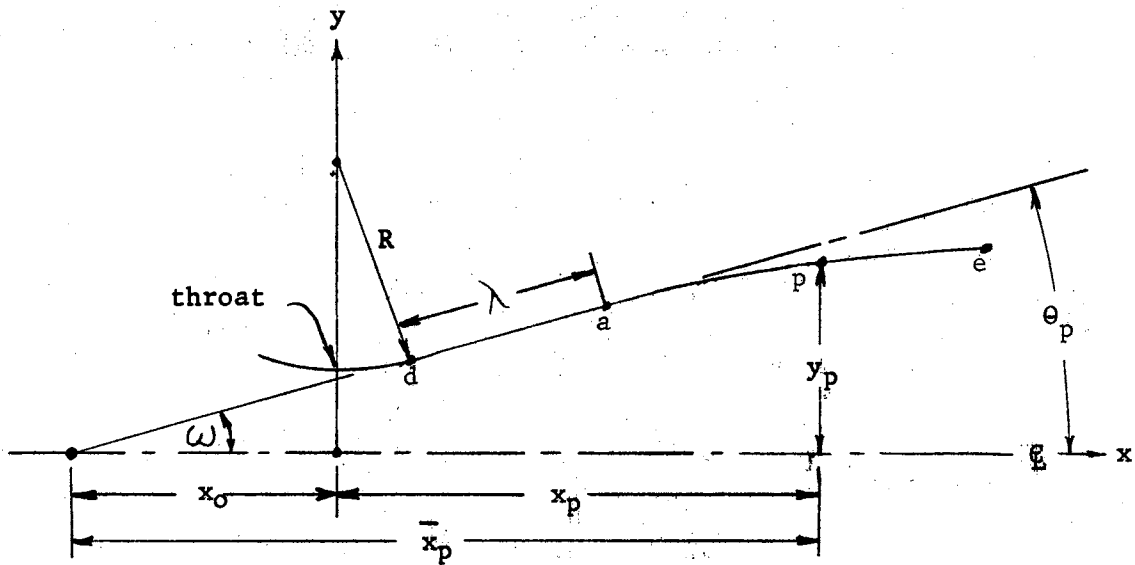


Figure 9. Foelsch Nozzle Details

TABLE II  
 PROPERTIES OF BOUNDARY MACH LINE FOR  $\gamma = 1.67$

M	$\sqrt{M^2-1}$	$\psi$	$\tau$
1.0050	0.10000	0.00711	1.00001
1.0112	0.15000	0.02377	1.00005
1.0198	0.20000	0.05562	1.00015
1.0308	0.25000	0.10690	1.00035
1.0440	0.30000	0.18115	1.00071
1.0595	0.35000	0.28122	1.00128
1.0770	0.40000	0.40923	1.00212
1.0966	0.45000	0.56651	1.00329
1.1180	0.50000	0.75372	1.00485
1.1413	0.55000	0.97085	1.00685
1.1662	0.60000	1.21737	1.00935
1.1927	0.65000	1.49223	1.01238
1.2207	0.70000	1.79404	1.01599
1.2500	0.75000	2.12110	1.02021
1.2806	0.80000	2.47151	1.02505
1.3124	0.85000	2.84322	1.03056
1.3454	0.90000	3.23414	1.03673
1.3793	0.95000	3.64212	1.04358
1.4142	1.00000	4.06505	1.05112

TABLE II (CONTINUED)

M	$\sqrt{M^2-1}$	$\psi$	$\tau$
1.4500	1.05000	4.50088	1.05935
1.4866	1.10000	4.94764	1.06827
1.5240	1.15000	5.40344	1.07787
1.5620	1.20000	5.86654	1.08816
1.6008	1.25000	6.33529	1.09912
1.6401	1.30000	6.80816	1.11074
1.6800	1.35000	7.28378	1.12303
1.7205	1.40000	7.76086	1.13596
1.7614	1.45000	8.23826	1.14953
1.8028	1.50000	8.71493	1.16372
1.8446	1.55000	9.18996	1.17853
1.8868	1.60000	9.66250	1.19394
1.9294	1.65000	10.13184	1.20994
1.9723	1.70000	10.59731	1.22651
2.0156	1.75000	11.05837	1.24366
2.0591	1.80000	11.51451	1.26135
2.1030	1.85000	11.96534	1.27960
2.1471	1.90000	12.41047	1.29837
2.1915	1.95000	12.84962	1.31767
2.2361	2.00000	13.28253	1.33748
2.2809	2.05000	13.70899	1.35779
2.3259	2.10000	14.12885	1.37860
2.3712	2.15000	14.54198	1.39988

TABLE II (CONTINUED)

M	$\sqrt{M^2-1}$	$\psi$	$\tau$
2.4166	2.20000	14.94829	1.42164
2.4622	2.25000	15.34770	1.44386
2.5080	2.30000	15.74019	1.46654
2.5539	2.35000	16.12575	1.48966
2.6000	2.40000	16.50436	1.51322
2.6462	2.45000	16.87606	1.53722
2.6926	2.50000	17.24090	1.56163
2.7391	2.55000	17.59891	1.58647
2.7857	2.60000	17.95016	1.61171
2.8324	2.65000	18.29474	1.63735
2.8792	2.70000	18.63271	1.66339
2.9262	2.75000	18.96418	1.68982
2.9732	2.80000	19.28923	1.71664
3.0203	2.85000	19.60798	1.74383
3.0676	2.90000	19.92052	1.77139
3.1149	2.95000	20.22695	1.79932
3.1623	3.00000	20.52741	1.82761
3.2098	3.05000	20.82199	1.85626
3.2573	3.10000	21.11081	1.88525
3.3049	3.15000	21.39398	1.91459
3.3526	3.20000	21.67163	1.94428
3.4004	3.25000	21.94387	1.97430
3.4482	3.30000	22.21080	2.00465
3.4961	3.35000	22.47255	2.03534

TABLE II (CONTINUED)

M	$\sqrt{M^2-1}$	$\psi$	$T$
3.5440	3.40000	22.72923	2.06634
3.5920	3.45000	22.98095	2.09767
3.6401	3.50000	23.22781	2.12931
3.6882	3.55000	23.46995	2.16127
3.7363	3.60000	23.70746	2.19353
3.7845	3.65000	23.94043	2.22611
3.8328	3.70000	24.16899	2.25898
3.8810	3.75000	24.39322	2.29215
3.9294	3.80000	24.61324	2.32562
3.9778	3.85000	24.82914	2.35938
4.0262	3.90000	25.04101	2.39344
4.0746	3.95000	25.24896	2.42777
4.1231	4.00000	25.45307	2.46240
4.1716	4.05000	25.65343	2.49730
4.2202	4.10000	25.85013	2.53248
4.2688	4.15000	26.04326	2.56794
4.3174	4.20000	26.23290	2.60367
4.3661	4.25000	26.41913	2.63967
4.4147	4.30000	26.60204	2.67594
4.4635	4.35000	26.78169	2.71248
4.5122	4.40000	26.95818	2.74928
4.5610	4.45000	27.13156	2.78634
4.6098	4.50000	27.30192	2.82366
4.6586	4.55000	27.46931	2.86123

TABLE II (CONTINUED)

M	$\sqrt{M^2-1}$	$\psi$	T
4.7074	4.60000	27.63382	2.89907
4.7563	4.65000	27.79551	2.93715
4.8052	4.70000	27.95444	2.97549
4.8541	4.75000	28.11068	3.01407
4.9031	4.80000	28.26428	3.05290
4.9520	4.85000	28.41531	3.09198
5.0010	4.90000	28.56383	3.13130
5.0500	4.95000	28.70990	3.17086
5.0990	5.00000	28.85355	3.21066



## APPENDIX B

### INSTRUMENT CALIBRATION

**Orifice.** The orifice calibration was carried out in accordance with the A. S. M. E. Power Test Codes on Flow Measurement. A schematic of the orifice calibration setup is shown in Fig. 10.

Water was used as the fluid to calibrate the orifice. The orifice calibration consisted of determining the flow coefficient by measuring the pressure differential across the orifice and by determining the flow rate of the water. The following equation was used to determine the flow coefficient of the orifice:

$$Q = KA_2 \sqrt{2g_c \rho \Delta P}$$

where

$Q$  = Volumetric flow rate, cfs.

$A_2$  = Area of orifice,  $\text{ft}^2$ .

$K$  = Flow coefficient

$\Delta P$  = Pressure differential across the orifice, psf.

$\rho$  = Density of the fluid,  $\text{lb}_m/\text{ft}^3$

$g_c$  =  $32.174 \text{ lb}_m\text{ft}/\text{lb}_f \text{ sec}^2$

The flow was regulated by the valve located downstream from the orifice. The valve upstream of the orifice was full open during the runs.

The flow rate was determined by diverting the flow of water into the weighing tank and measuring, with an electric timer, the time required

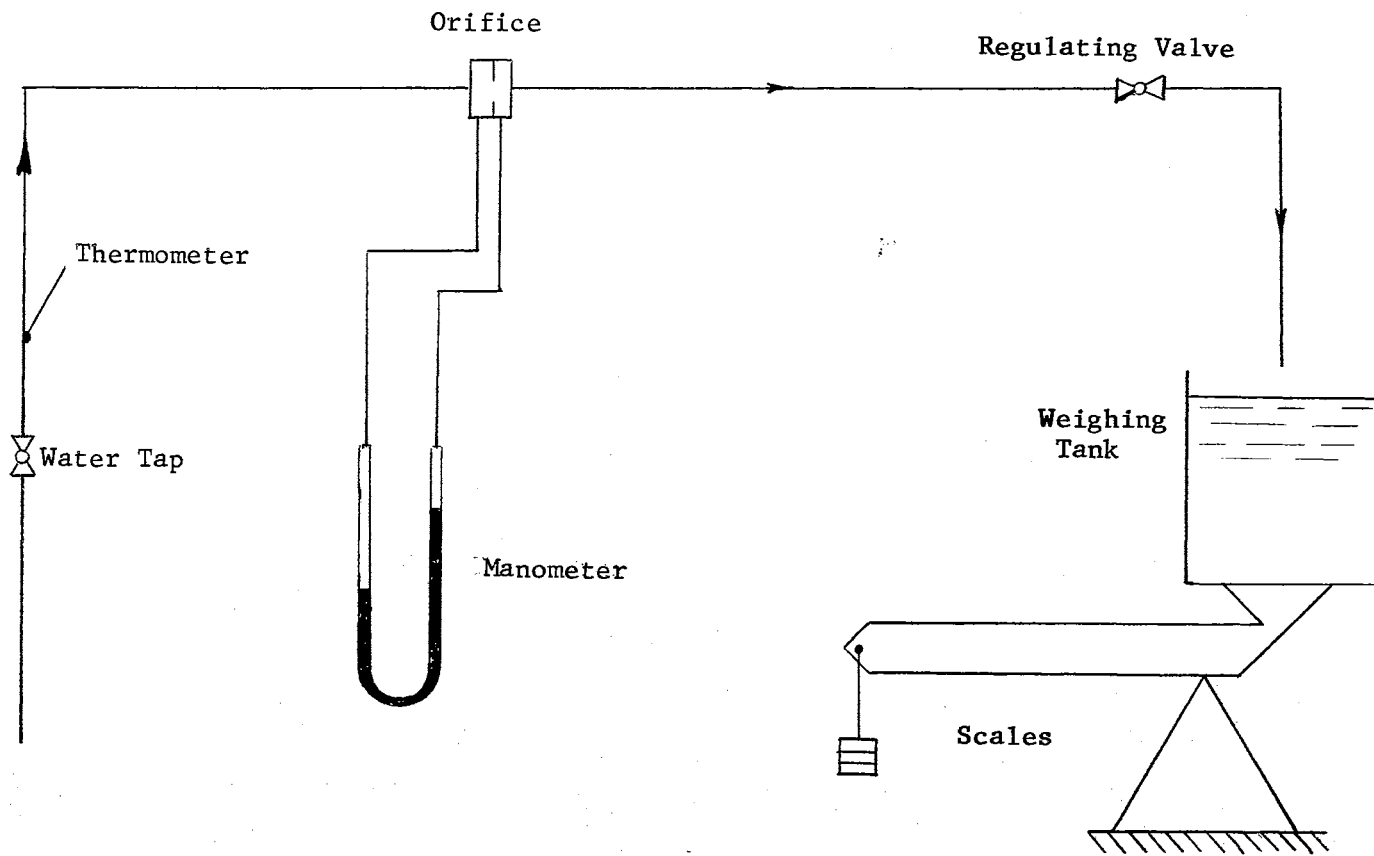


Figure 10. Orifice Calibration Setup

for a specified weight of water to flow into the tank. By knowing the weight of water and the time, the flow rate was calculated.

The temperature of the water was measured upstream from the orifice. Any variation of the water temperature between this location and the orifice was considered negligible. The properties of the water were determined at this temperature.

The pressure differential across the orifice was determined by connecting the pressure taps on the orifice flanges to a U-tube manometer. Mercury was used for the manometer fluid.

Seven runs were made. The flow corresponded to Reynolds numbers from  $5 \times 10^4$  to  $2.2 \times 10^5$ . The flow coefficient and the Reynolds number were calculated for each run. These values are plotted as flow coefficient versus Reynolds number in Fig. 11.

The orifice was used to measure the flow of air to the supersonic nozzle during testing. The flow coefficient corresponding to the appropriate Reynolds number was used to determine the flow rate of the air.

**Pressure Gages.** The pressure gages used for measuring the air pressure at the orifice and the air pressure in the mixing chamber were calibrated using a dead weight tester.

The gages were tested by adding weights in 5 psi increments from 0 to 100 psi. Readings were taken as each weight was added and as each weight was taken off the tester. An average of the two readings was assumed to be the correct reading on each gage. The calibration curves of pressure reading versus correction for both gages are shown in Fig. 12.

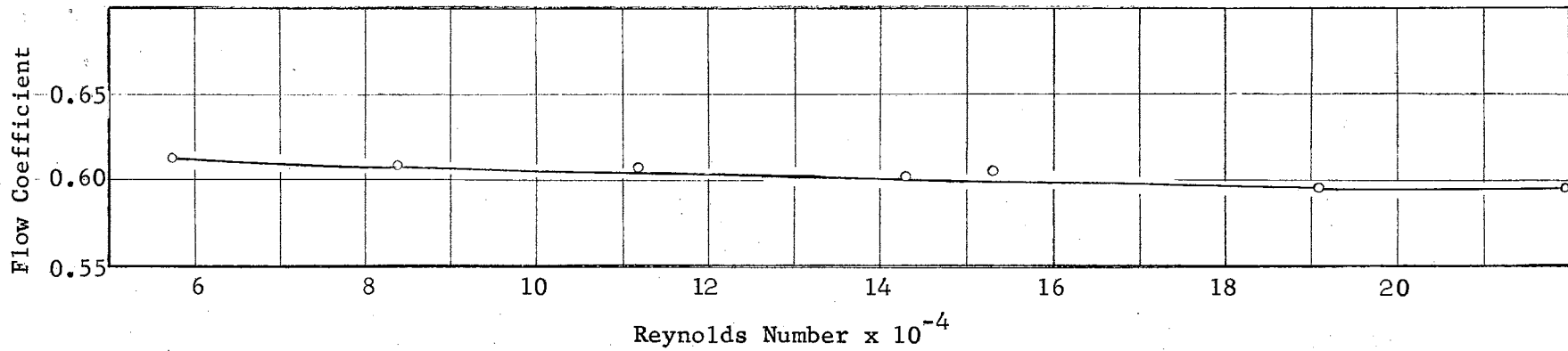


Figure 11. Orifice Calibration Curve

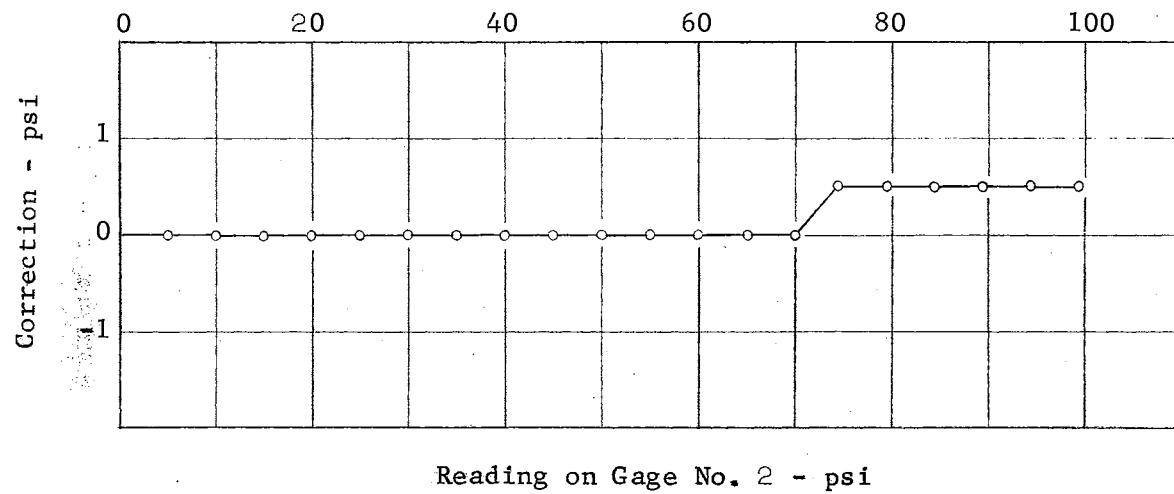
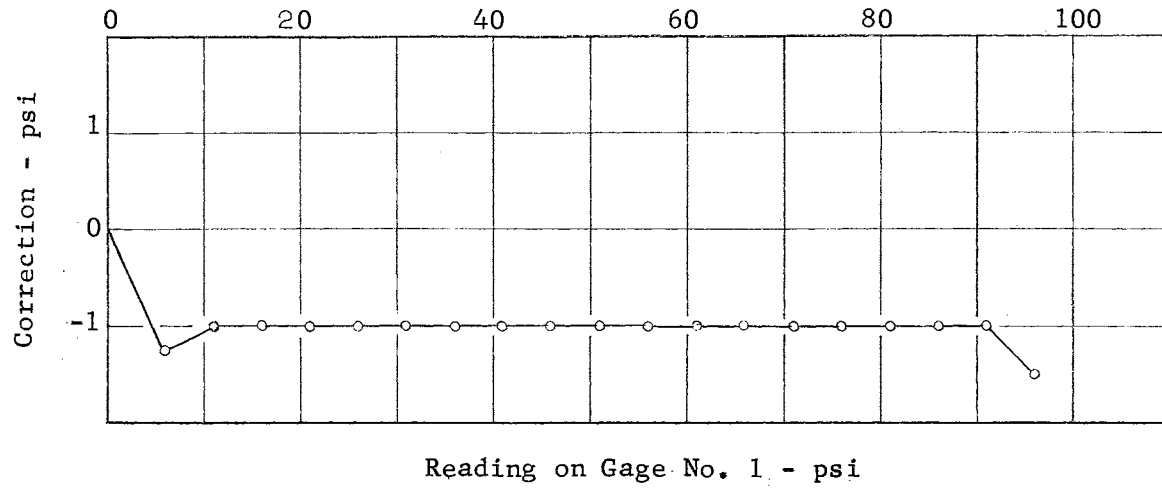


Figure 12. Pressure Gage Calibration Curves

VITA

Merle Keith Burkhart

Candidate for the Degree of

Master of Science

Thesis: A SUPERSONIC, SHOCK FREE NOZZLE FOR AN EXISTING PLASMA GENERATOR AND ITS FACILITIES

Major Field: Mechanical Engineering

Biographical:

Personal Data: Born near Quinlan, Oklahoma, September 30, 1933, the son of Vernie Ray and Louisa Mae Burkhart.

Education: Graduated from Freedom High School, Freedom, Oklahoma in May, 1951. Entered Oklahoma State University in January, 1952 and discontinued schooling in January, 1953. Re-entered Oklahoma State University in January, 1956 and received the Bachelor of Science Degree in Mechanical Engineering in May, 1959; completed requirements for the Master of Science Degree in August, 1960.

Experience: Served from June, 1953 to May, 1955 in the United States Army. Worked as a Junior Engineer for Shell Pipe Line Corporation during the summer of 1958. Worked as an engineer for Magnolia Field Research Laboratory during the summer of 1959.

Professional Organizations: Member of the American Society of Mechanical Engineers. Presently enrolled as an Engineer-in-Training with the State Board of Registration for Professional Engineers in Oklahoma.